



Published in final edited form as:

Eur Radiol. 2016 January ; 26(1): 103–113. doi:10.1007/s00330-015-3812-2.

Radiologic-pathologic analysis of quantitative 3D tumour enhancement on contrast-enhanced MR imaging: a study of ROI placement

Arun Chockalingam¹, Rafael Duran¹, Jae Ho Sohn¹, Rüdiger Schernthaler¹, Julius Chapiro¹, Howard Lee¹, Sonia Sahu¹, Sonny Nguyen¹, Jean-François Geschwind¹, and MingDe Lin²

Arun Chockalingam: chocka@rpi.edu; Rafael Duran: rafaelduran.md@gmail.com; Jae Ho Sohn: sohn87@gmail.com; Rüdiger Schernthaler: rschern1@jhmi.edu; Julius Chapiro: j.chapiro@googlemail.com; Howard Lee: mail2howielee@gmail.com; Sonia Sahu: soniapsahu@gmail.com; Sonny Nguyen: sonnytrnguyen@gmail.com; Jean-François Geschwind: jfg@jhmi.edu; MingDe Lin: ming.lin@philips.com

¹Russell H. Morgan Department of Radiology and Radiological Science, Division of Vascular and Interventional Radiology, The Johns Hopkins Hospital, Sheikh Zayed Tower, Ste 7203, 1800 Orleans St, Baltimore, MD 21287, USA

²U/S Imaging and Interventions (UII), Philips Research North America, Briarcliff Manor, NY, USA

Abstract

Objectives—To investigate the influence of region-of-interest (ROI) placement on 3D tumour enhancement [Quantitative European Association for the Study of the Liver (qEASL)] in hepatocellular carcinoma (HCC) patients treated with transcatheter arterial chemoembolization (TACE).

Methods—Phase 1: 40 HCC patients had nine ROIs placed by one reader using systematic techniques (3 ipsilateral to the lesion, 3 contralateral to the lesion, and 3 dispersed throughout the liver) and qEASL variance was measured. Intra-class correlations were computed. Phase 2: 15 HCC patients with histosegmentation were selected. Six ROIs were systematically placed by AC (3 ROIs ipsilateral and 3 ROIs contralateral to the lesion). Three ROIs were placed by 2 radiologists. qEASL values were compared to histopathology by Pearson's correlation, linear regression, and median difference.

Results—Phase 1: The dispersed method (abandoned in phase 2) had low consistency and high variance. Phase 2: qEASL correlated strongly with pathology in systematic methods [Pearson's

Correspondence to: Jean-François Geschwind, jfg@jhmi.edu.

All other authors do not have any conflicts of interest to disclose.

Electronic supplementary material The online version of this article (doi:10.1007/s00330-015-3812-2) contains supplementary material, which is available to authorized users.

Institutional Review Board approval was obtained. Written informed consent was waived by the Institutional Review Board.

Our study follows our recently published manuscript to *European Radiology* where qEASL was shown to predict survival in patients with colorectal metastases to the liver better than the uni-dimensional and bi-dimensional measurements (mRECIST, RECIST, WHO, EASL): Julius Chapiro, Rafael Duran, MingDe Lin, et al. (2015) *Early Survival Prediction after Intra-arterial Therapies: A 3D quantitative MRI assessment of Tumour Response after TACE or Radioembolization of Colorectal Cancer Metastases to the Liver.* *Eur Radiol* DOI 10.1007/s00330-015-3595-5.

Methodology: retrospective, experimental, performed at one institution.

correlation coefficient=0.886 (ipsilateral) and 0.727 (contralateral)] and in clinical methods (0.625 and 0.879). However, ipsilateral placement matched best with pathology (median difference: 5.4 %; correlation: 0.89; regression CI: [0.904, 0.1409]).

Conclusions—qEASL is a robust method with comparable values among tested placements. Ipsilateral placement showed high consistency and better pathological correlation.

Keywords

Tumour segmentation; MRI; Hepatocellular carcinoma; TACE; ROI

Introduction

Hepatocellular carcinoma (HCC) represents a growing public health problem worldwide, with more than 800,000 newly diagnosed cases a year. HCC is the most commonly diagnosed primary liver cancer [1], and is estimated to cause over half a million deaths per year worldwide [2]. Most patients are non-surgical candidates and interventional image-guided treatments (IGT) are often the best suitable therapy [3].

Transarterial chemoembolization (TACE) is a type of IGT, which is considered the standard of care for intermediate-stage HCC [3–5]. Accurate assessment of tumour response after TACE is a fundamental parameter that influences future treatment cycles and thus patient management. However, currently available imaging biomarkers such as Response Evaluation Criteria in Solid Tumours (RECIST), European Association of the Study of the Liver guidelines (EASL), and modified RECIST (mRECIST) were shown to have limitations in relation to pathological correlation, patient survival prediction, and inter-reader agreement [6–10]. To address the limitations of these one-dimensional and two-dimensional qualitative approaches, a 3D quantitative tumour enhancement (qEASL) was developed [11]. qEASL is calculated by measuring the volume of enhancing regions within the tumour compared to the total volume of the lesion. This novel quantitative technique has been shown to have a strong positive correlation with 3D pathological measurements and survival after TACE and strong inter-reader correlation [6, 7, 11–13].

In order to calculate qEASL values, a lesion is first segmented in 3D and then a region-of-interest (ROI) is placed in healthy, non-enhancing liver tissue as a reference in order to measure the volume of tumour showing greater relative enhancement [11]. Thus, ROI placement is a critical step for accurate tumour response assessment. Furthermore, it has been shown that ROI placement in general may be subject to high variance due to heterogeneities inherent to the measured structure/organ or imaging artefacts [14, 15]. Because the ROI placement in qEASL could be defined in any region of the liver, the variability of qEASL could potentially be high. If qEASL is to be used in determining clinical prognosis and decision making, there must be a set of guidelines for which qEASL can be implemented accurately and precisely.

The purpose of our study was to investigate the reproducibility and validity (via pathological correlation) of different ROI placement methods when measuring 3D tumour enhancement

(qEASL) in HCC patients treated with TACE in order to identify the most suitable method for ROI placement.

Materials and methods

This retrospective, single-institution study was conducted in compliance with the Health Insurance Portability and Accountability Act and approved by the Institutional Review Board. Informed consent was waived. The design of the study was in agreement with the Standards for Reporting of Diagnostic Accuracy guidelines [16].

Phase 1: Impact of ROI placement method on qEASL values

Study cohort—From January to December 2013, 68 patients with HCC underwent a TACE procedure for the first time at our institution [17]. Twenty-one patients were excluded for the following reasons: absence of contrast-enhanced magnetic resonance imaging (CE-MRI) after TACE ($n = 16$), CE-MRI with motion artefacts ($n = 4$) and infiltrative-type HCC ($n=8$). Thus, the final study cohort consisted of 40 patients. The patient baseline characteristics are shown in Table 1.

MR imaging technique—All patients underwent a standardized MR imaging liver protocol 4–6 weeks after initial TACE. MR imaging was performed on a 1.5 Tesla scanner (Siemens Magnetom Avanto, Erlangen, Germany) using a phased array torso coil. The protocol included 1) axial T2-weighted fast spin echo images (repetition time/echo time, 5000/100 milliseconds; matrix size, 256×256; section thickness, 8 mm; intersection gap, 2 mm; receiver bandwidth, 32 kHz); 2) axial T1-weighted dual fast gradient recalled echo sequence; and 3) axial breath-hold unenhanced and contrast-enhanced [0.1 mmol per kilogram of body weight of intravenous gadodiamide (Omniscan; GE Healthcare, Princeton, NJ)] T1-weighted three-dimensional fat-suppressed spoiled gradient recalled echo images (5.1/1.2; field of view, 320–400 mm; matrix size, 192×160; section thickness, 4–6 mm; receiver bandwidth, 64 kHz; flip angle, 15°) in the arterial, portal venous, and equilibrium phases (20 seconds, 60–70 seconds, and 180–200 seconds after intravenous contrast material injection, respectively) [6].

TACE protocol—Briefly, using the Seldinger technique, access was gained in the common femoral artery. The celiac axis was then catheterized using a 5-F Simmons-1 catheter (Cordis, Miami Lakes, FL) through which a 2.8 F Renegade HI-FLO microcatheter (Boston Scientific, Marlborough, MA) was coaxially advanced. Several angiographic steps were performed to define the hepatic arterial anatomy and determine tumour localization and portal venous patency. Selective injection rates were adapted to the calibre of the blood vessels and ranged from 1 to 3 mL/sec. After good microcatheter positioning was confirmed, the drug payload [for conventional TACE (cTACE), drug-eluting beads TACE (DEB-TACE)] was delivered. For cTACE ($n=8$), Lipiodol (Guerbet, France) was mixed 1:1 with a solution containing 50 mg of doxorubicin and 10 mg of mitomycin-C. This injection was followed by the administration of bland microspheres with a diameter of 100–300 µm (Embospheres, Merit Medical, USA). For DEB-TACE ($n=7$), a 4 mL solution of DC Beads (Biocompatibles/BTG, Surrey, United Kingdom) with a diameter of 100–300 µm were

loaded with 100 mg of doxorubicin hydrochloride (25 mg/mL) and mixed with 4 mL of iodinated contrast medium (Oxilan 350, Guerbet).

Semiautomatic tumour segmentation & ROI placement—A quantitative tumour segmentation software (Medisys, Philips Research, Suresnes, France), based on non-Euclidean geometry and the theory of radial basis function, was used to segment target lesions in 3D and calculate their respective volumes. Previous studies have shown that this semiautomatic segmentation method can accurately segment in 3D and has high reproducibility [10, 12, 13]. It is a fully interactive process that allows for the user to define an initial control point and to expand the volume in 3D by mouse click and drag to the tumour boundary. This system permits user input and corrections at all steps of the process [8]. Semiautomatic tumour segmentation was performed on the MR images by a radiologist (RS). Each lesion outlined using this tool was located in a 3D region where centre and size were defined by the user (interactively, this information is given by a mouse click followed by a mouse drag). An example of the segmentation outline and 3D rendering produced is shown in Fig. 1.

Calculation of 3D tumour enhancement (qEASL) was performed using a software prototype (Medisys, Philips Research, Suresnes, France), as previously described in detail [11]. Briefly, the difference between pre-contrast and CE-MRI acquired 20 seconds after injection of contrast is used for qEASL measurements (Fig. 1). Viable enhancing tumour was defined as voxels where enhancement is higher (greater than two standard deviations of the reference ROI value) than enhancement of the healthy liver parenchyma [3, 18, 19]. The largest lesion (when multiple lesions were present) was evaluated for each patient. ROI placements were performed by a reader (AC, undergraduate biomedical engineer who was trained to use the software prototype). The reader used a systematic approach to place the ROIs in healthy liver tissue such that three ROIs were placed near the lesion (in the ipsilateral liver lobe), three ROIs in the contralateral liver lobe, and three ROIs dispersed throughout the liver. In the latter method, for example, if there was a lesion in the posterior sector of the right liver lobe, a ROI would be placed within the posterior segments (VI and VII), the anterior segments (V and VIII), and the left liver segments (II, III, and IV). For each ROI placement, care was taken to avoid blood vessels, liver periphery, the gallbladder, and motion artefacts. An example of the systematic placement of ROIs is shown in Fig. 2. One month later, this experiment was replicated in order to examine temporal consistency.

Statistical analysis

Descriptive statistics were used to summarize the data. Mean and range were used for continuous variables, while frequencies and percent were used for categorical variables. Intra-rater consistency, inter-method consistency, and inter-temporal consistency (consistency of measurement at two different time points) in qEASL values were assessed with intra-class correlation coefficient (ICC). This is a true index of intra-rater consistency, in contrast to the conventional Pearson's product moment correlation, which is a measure of linear association. Single measure ICCs were derived from a one-way, random, and absolute agreement model. Variance for each method (calculated within each patient) was also calculated and plotted. Analysis was performed in R version 3.1.1 (Vienna, Austria: R

Foundation for Statistical Computing, 2014) and SPSS version 22.0 (Armonk, NY: IBM Corp: IBM SPSS Statistics for Windows, 2013).

Phase 2: radiological–pathological correlation of qEASL values

Study cohort—From 2007 to 2012, 20 patients with HCC from our database [17] were treated with TACE at our institution as a bridge to surgical treatment (hepatic resection or liver transplant), and had complete quantitative pathological analysis of the target lesion. As an inclusion criterion, less than 90 days should have passed between MR examination and surgery for these patients. Five patients were excluded due to inadequate MR imaging quality, leaving the final study cohort to be 15. The patient baseline characteristics are shown in Table 1.

Histopathological evaluation—The radiologically selected lesions were matched with gross pathology descriptions of the specimen by an experienced liver pathologist who was blinded to the imaging results. As described more thoroughly in a previous radiological–pathological study, 0.5–1.0 cm sections of the treated index lesions were taken (according to our institutional protocol of serial liver sectioning) and prepared into slides using haematoxylin and eosin staining [7]. For histosegmentation, the slides were digitalized (20× magnification) using a high-resolution system (Aperio, Vista, California, USA), and then assessed using the Aperio ImageScope Software. Segmentation of necrotic as well as total tumour areas was done manually, slide-by-slide, by the pathologist in order to obtain 3D quantitative data of the whole lesion. The ratio of identified necrotic and viable areas was expressed as calculated percentage [7] (Fig. 3). MR imaging after TACE and prior to resection was used for qEASL analysis.

MR imaging technique, semiautomatic tumour segmentation & ROI placement

—Tumour segmentation and ROI placement were performed using the same software prototypes and technique described in phase 1. The same Gd-enhanced MR sequence from phase 1 was used in this phase. Two experienced radiologists RS and RD (8 years of experience and 7 years of experience, respectively) placed ROIs while the reader (AC) from phase 1 systematically placed six ROIs (three in the ipsilateral liver lobe and three in the contralateral liver lobe to the lesion). The readers were blinded to the pathological results. In order to allow direct comparison with the pathological analysis, which quantified the amount of necrosis present in the tumours, the percentage of enhancing voxels in qEASL was subtracted from 100 percent.

Statistical analysis—Median difference with standard deviation between the systematic and clinical placement methods and pathology were calculated. Pearson's correlation coefficients between each ROI method and pathology were computed. Linear regression was created to investigate the relationship between percent tumour necrosis from pathology and percent tumour enhancement according to qEASL. Confidence intervals (CIs) of the regression coefficients were constructed and plotted along with the identity line, which represents perfect agreement between qEASL and pathology. These analyses were performed in R version 3.1.1 (Vienna, Austria: R Foundation for Statistical Computing, 2014).

Results

Phase 1: impact of ROI placement on qEASL values

Twenty-nine out of forty patients (72.5 %) had tumours in the right lobe. The mean tumour volume was 146.9 cm³ (standard deviation 420.9; range 1.2–2516.4). Supporting Table S1 of the Appendix summarizes tumour location and mean qEASL values (from each ROI placement method) for each patient. For ipsilateral ROI placement, the mean qEASL percentage was 32.8 (standard deviation 25.3; range 0–80.7). For contralateral ROI placement, the mean qEASL percentage was 39.9 (standard deviation 31.0; range 0–100). For ROIs dispersed in the liver, the mean qEASL percentage was 37.6 (standard deviation 24.8; range 0–92.9). A matrix showing intra-class correlation between qEASL percentages obtained from the different methods is shown in Table 2. The highest ICC coefficient was seen in the contralateral method (0.971), and the lowest was seen in the dispersed method (0.604). Variance of qEASL values for each method used was also calculated and plotted in Fig. 4. High variance in the dispersed method was observed (as high as 2800). Variances in the ipsilateral and contralateral methods were much lower (reaching only 1100 and 200, respectively).

Phase 2: radiological-pathological correlation of qEASL values

Thirteen out of 15 patients (87 %) had tumours in the right lobe. The mean percent necrosis determined by pathology was 71.0 (standard deviation 34.9; range 5.26–100). The mean interval between MR imaging and surgery was 34 days (range, 2–83 days). Only ipsilateral and contralateral methods were tested because of the low variance and high intra-class correlation seen in phase 1. The calculated mean qEASL percent necrosis for the ipsilaterally and contralaterally placed ROIs (AC) were 79.1 (standard deviation 6.8; range 35.5–100.0) and 65.5 (standard deviation 5.0; range 0.1–100.0), respectively. For the ROIs placed by radiologists RS and RD, the mean qEASL percent necrosis was 86.6 (standard deviation 8.7; range 65.7–100.0) and 77.6 (standard deviation 3.5; range 13.2–100.0), respectively. Average percent necrosis (qEASL percentage subtracted from 100 %) calculated using the systematic and clinical methods of ROI placement are reported in Table 3. Using a simple linear model, the regression coefficients for the ipsilateral, contralateral, and radiologists ROI placements were calculated (Table 4). The identity line is contained within the 95 % CI for ipsilateral placement, as shown in Fig. 5. Pearson's correlation coefficients between pathology and the ipsilateral and contralateral methods were 0.886 and 0.727, respectively. Pearson correlation coefficients and median differences comparing placement methods to pathology are also shown in Table 4.

Discussion

The main finding of our study is that the ipsilateral and contralateral ROI placement methods demonstrated high intrarater consistency and low variance with respect to qEASL values as well as strong correlation with pathology, highlighting the accuracy of the 3D quantitative tumour response assessment. Of the two ROI placement methods, the ipsilateral approach demonstrated the best correlation with pathology as well as intra-reader and temporal consistency.

Radiologic assessment of tumour enhancement is widely used and accepted as a surrogate biomarker for outcome endpoints in most cancer-related clinical trials. Thus, it is critical to accurately evaluate therapy response (change in qEASL percentage) to make informed decisions regarding the best available treatment options.

In our study, ROIs were placed systematically in groups of three at two different time points, allowing for a more comprehensive analysis. Phase 1 assessed precision of ROI placement methods with one reader, while phase 2 assessed accuracy of these techniques with three readers using comparison with pathology. From statistical analysis, the ipsilateral ROI placement had a stronger correlation with pathology than the contralateral ROI placement (0.886 and 0.727, respectively). We suspect that this holds true due to different signal intensities throughout the nontumoral liver parenchyma caused by magnetic field heterogeneities. In one study, Mitsufuji et al. [20] tested inter-observer and intra-observer consistency of liver stiffness measurement on MR elastography by varying ROI shape (circular or free-hand drawn) and images where ROIs were placed (fused images of MRE and anatomical images). They concluded that ROIs should only be placed in the right lobe due to motion artefacts in the left lobe. In another study, Mürtz et al. [15] conducted MR diffusion measurements of the abdomen using diffusion-weighted single-shot sequence with and without pulse triggering. They identified diffusion-weighted MR imaging motion artefacts that are present due to the pulsatile motion of the aorta. Reeder et al. [21] acknowledge MRI field heterogeneities and discuss decomposition methods to measure a field map and demodulate this noise from the signal. Taken together, these results indicate that clinicians using qEASL should place ROIs ipsilateral to the lesion to not only decrease variability of the qEASL value but also to increase the accuracy of the measurements by accounting for cardiac motion artefacts.

Given the heterogeneous appearance of the liver, especially with a background of cirrhosis, the technique used and the observer are important factors for ROI placement. Aspects such as work load, level of experience, fatigue, and personal reading approach play an important role in the interpretation of images and more specifically in the placement of ROIs [22]. Other works also showed the effect of ROI placement on observational factors such as inter-reader variability [23–26] and semi-automatic tumour segmentation [27].

There were some limitations to our study. In phase 1, patients did not have histological workup of complete lesions, so there was no ground truth that qEASL values could be compared to. However, the purpose of this portion of our study was to establish a baseline for the systematic methods and to test their reproducibility. This would help us streamline our radiologic-pathologic analysis, which is the focal point of our study. In phase 2, our sample size for the radiological-pathological analysis was relatively small because pathological assessment requires thorough histological workup of the complete lesion (after resection or liver transplantation) [7]. For this reason, patients with incompletely preserved lesions could not be included in the patient pool of interest. Patients with lesions greater than 7.5 cm in size were also not considered because we could not evaluate gross pathology on tumour explants, given the retrospective element of our study. Because TACE induces tumour necrosis via a unique mechanism [7], patients treated with other intra-arterial therapies (i.e., Yttrium-90 radioembolization and ablative techniques) were excluded from

histosegmentation. These circumstances greatly limited our choice of patients for analysis. However, our cohort ($n=15$) size was still comparable to other work correlating imaging findings with pathology [28]. Second, the pathology was obtained from surgical candidates who generally had less advanced liver disease compared to the overall cirrhotic patient population. Thus, the results of the present study need to be confirmed in another study with a more globally representative cohort. Third, our study did not use bolus tracking. Because a fixed time delay (20s) for arterial phase imaging was used, there could be a variety of arterial bolus delay time, and this could affect the enhancement of the lesions [29]. Specifically, there could be inherent inconsistency of the arterial contrast enhancement. Usually, when the total amount of contrast medium is determined based on body weight, either bolus tracking method should be used, or at least injection duration must be kept constant [29]. However, in our institution, a fixed timing acquisition protocol that is common for liver imaging is used to visualize lesions and healthy parenchyma [30]. The local transit time inside the liver, due to embolic effects of TACE, will be different from that between the aorta and liver at baseline and on follow-up imaging. So, a bolus tracking method may not produce significant improvement in the qEASL values. Fourth, well-differentiated or poorly differentiated HCC could show vascularity similar to that of the surrounding non-tumorous liver tissue, and thus may have been overlooked. However, the definition of viable enhancing tumour used in our study followed recognized guidelines [3, 18, 19].

In conclusion, our study demonstrated that qEASL values calculated using ipsilateral ROI placement matched well with pathology. Placing ROIs in the ipsilateral liver lobe of the lesion would produce results that are consistent and most importantly, strongly correlate with pathology. This finding can serve as a guideline for future 3D quantitative studies using qEASL as a surrogate biomarker of tumour response.

Supplementary Material

Refer to Web version on PubMed Central for supplementary material.

Acknowledgments

The scientific guarantor of this publication is Jean-François Geschwind. The authors of this manuscript declare relationships with the following companies: Dr. Geschwind reports grants from NIH, grants from Philips Medical, during the conduct of the study; personal fees from Consultant to Nordion, personal fees from Consultant to Biocompatibles/BTG, personal fees from Consultant to Bayer HealthCare, grants from DOB, grants from Biocompatibles/BTG, grants from Bayer HealthCare, grants from Nordion, grants from Context Vision, grants from SIR, grants from RSNA, grants from Guerbet, outside the submitted work. Dr. Lin reports grants from NIH, during the conduct of the study; and is a Philips employee.

Our study has received funding by NIH/NCI R01 CA160771, P30 CA006973, Philips Research North America, Briarcliff Manor, NY, USA.

References

1. Siegel RMJ, Zou Z, Jemal A. Cancer statistics. *CA Cancer J Clin.* 2014; 64:9–29. [PubMed: 24399786]
2. Chockalingam APC. Battle of the bulge and the burden of gastrointestinal cancers. *Pract Gastroenterol.* 2013; XXXVII:15–24.

3. European Association For The Study Of The L, European Organisation For R, Treatment Of C. EASL-EORTC clinical practice guidelines: management of hepatocellular carcinoma. *J Hepatol.* 2012; 56:908–943. [PubMed: 22424438]
4. Lo CM, Ngan H, Tso WK, et al. Randomized controlled trial of transarterial lipiodol chemoembolization for unresectable hepatocellular carcinoma. *Hepatology.* 2002; 35:1164–1171. [PubMed: 11981766]
5. Llovet JM, Real MI, Montana X, et al. Arterial embolisation or chemoembolisation versus symptomatic treatment in patients with unresectable hepatocellular carcinoma: a randomised controlled trial. *Lancet.* 2002; 359:1734–1739. [PubMed: 12049862]
6. Duran R, Chapiro J, Frangakis C, et al. Uveal melanoma metastatic to the liver: the role of quantitative volumetric contrast-enhanced MR imaging in the assessment of early tumor response after transarterial chemoembolization. *Transl Oncol.* 2014; 7:447–455. [PubMed: 24953419]
7. Chapiro J, Wood LD, Lin M, et al. Radiologic-pathologic analysis of contrast-enhanced and diffusion-weighted MR imaging in patients with HCC after TACE: diagnostic accuracy of 3D quantitative image analysis. *Radiology.* 2014; 273:746–758. [PubMed: 25028783]
8. Chapiro J, Lin M, Duran R, Scherthaner RE, Geschwind JF. Assessing tumor response after loco-regional liver cancer therapies: the role of 3D MRI. *Expert Rev Anticancer Ther.* 2014; 10:1586–1597. [PubMed: 25171402]
9. Takeda H, Osaki Y, Inuzuka T, Nakajima J, Matsuda F, Sakamoto A, Hatamaru K, Henmi S, Ishikawa T, Saito S, Nishikawa H, Kita R, Kimura T. Appropriateness and limitations of modified response evaluation criteria in solid tumors (mRECIST) in evaluating the efficacy of molecular-targeted therapy for patients with hepatocellular carcinoma. *Jpn Soc Hepatol Kanzo.* 2012; 53:147–154.
10. Chapiro J, Duran R, Lin MingDe, Scherthaner Rüdiger, Lesage David, Wang Zhijun, Savic Lynn Jeannette, Geschwind Jean-François. Early Survival Prediction after Intraarterial Therapies: A 3D quantitative MRI assessment of Tumor Response after TACE or Radioembolization of Colorectal Cancer Metastases to the Liver. *Eur Radiol.* 2014 Epub ahead of print.
11. Lin M, Pellerin O, Bhagat N, et al. Quantitative and volumetric european association for the study of the liver and response evaluation criteria in solid tumors measurements: feasibility of a semiautomated software method to assess tumor response after transcatheter arterial chemoembolization. *J Vasc Interv Radiol.* 2012; 23:1629–1637. [PubMed: 23177109]
12. Pellerin O, Lin M, Bhagat N, Ardon R, Mory B, Geschwind JF. Comparison of semi-automatic volumetric VX2 hepatic tumor segmentation from cone beam CT and multi-detector CT with histology in rabbit models. *Acad Radiol.* 2013; 20:115–121. [PubMed: 22947274]
13. Tacher V, Lin M, Chao M, et al. Semiautomatic volumetric tumor segmentation for hepatocellular carcinoma: comparison between C-arm cone beam computed tomography and MRI. *Acad Radiol.* 2013; 20:446–452. [PubMed: 23498985]
14. Viviani R. Unbiased ROI selection in neuroimaging studies of individual differences. *Neuroimage.* 2010; 50:184–189. [PubMed: 19900563]
15. Murtz P, Flacke S, Traber F, van den Brink JS, Gieseke J, Schild HH. Abdomen: diffusion-weighted MR imaging with pulse-triggered single-shot sequences. *Radiology.* 2002; 224:258–264. [PubMed: 12091693]
16. Bossuyt PM, Reitsma JB, Bruns DE, et al. The STARD statement for reporting studies of diagnostic accuracy: explanation and elaboration. *Ann Intern Med.* 2003; 138:W1–W12. [PubMed: 12513067]
17. Lee H, Chapiro J, Scherthaner R, Duran R, Wang Z, Gorodetski B, Geschwind J-F, Lin M. How I do it: a practical database management system to assist clinical research teams with data collecting, organization, and reporting. *Acad Radiol.* 2015; 22:527–533. [PubMed: 25641319]
18. Bruix J, Sherman M, Llovet JM, et al. Clinical management of hepatocellular carcinoma. Conclusions of the Barcelona-2000 EASL conference. European association for the study of the liver. *J Hepatol.* 2001; 35:421–430. [PubMed: 11592607]
19. Lencioni R, Llovet JM. Modified RECIST (mRECIST) assessment for hepatocellular carcinoma. *Semin Liver Dis.* 2010; 30:52–60. [PubMed: 20175033]

20. Mitsufuji T, Shinagawa Y, Fujimitsu R, et al. Measurement consistency of MR elastography at 3.0 T: comparison among three different region-of-interest placement methods. *Jpn J Radiol.* 2013; 31:336–341. [PubMed: 23456548]
21. Reeder SB, Cruite I, Hamilton G, Sirlin CB. Quantitative assessment of liver Fat with magnetic resonance imaging and spectroscopy. *J Magn Reson Imaging.* 2011; 34:729–749. [PubMed: 21928307]
22. Heye T, Merkle EM, Reiner CS, et al. Reproducibility of dynamic contrast-enhanced MR imaging Part II. Comparison of intra- and interobserver variability with manual region of interest placement versus semiautomatic lesion segmentation and histogram analysis. *Radiology.* 2013; 266:812–821. [PubMed: 23220891]
23. Tomaru Y, Inoue T, Oriuchi N, Takahashi K, Endo K. Semi-automated renal region of interest selection method using the double-threshold technique: inter-operator variability in quantitating ^{99m}Tc-MAG3 renal uptake. *Eur J Nucl Med.* 1998; 25:55–59. [PubMed: 9396875]
24. Sattarivand M, Caldwell C, Poon I, Soliman H, Mah K. Effects of ROI placement on PET-based assessment of tumor response to therapy. *Int J Mol Imaging.* 2013; 2013:132804. [PubMed: 23533749]
25. Habte F, Budhiraja S, Keren S, Doyle TC, Levin CS, Paik DS. In situ study of the impact of inter- and intra-reader variability on region of interest (ROI) analysis in preclinical molecular imaging. *Am J Nucl Med Mol Imaging.* 2013; 3:175–181. [PubMed: 23526701]
26. Cutajar M, Mendichovszky IA, Tofts PS, Gordon I. The importance of AIF ROI selection in DCE-MRI renography: reproducibility and variability of renal perfusion and filtration. *Eur J Radiol.* 2010; 74:e154–e160. [PubMed: 19541441]
27. Levman J, Warner E, Causer P, Martel A. Semi-automatic region-of-interest segmentation based computer-aided diagnosis of mass lesions from dynamic contrast-enhanced magnetic resonance imaging based breast cancer screening. *J Digit Imaging.* 2014; 27:670–678. [PubMed: 25091735]
28. Vouche M, Kulik L, Atassi R, et al. Radiological-pathological analysis of WHO, RECIST, EASL, mRECIST and DWI: Imaging analysis from a prospective randomized trial of Y90 +/- sorafenib. *Hepatology.* 2013; 58:1655–1666. [PubMed: 23703789]
29. Shinozaki K, Yoshimitsu K, Irie H, et al. Comparison of test-injection method and fixed-time method for depiction of hepatocellular carcinoma using dynamic steady-state free precession magnetic resonance imaging. *J Comput Assist Tomogr.* 2004; 28:628–634. [PubMed: 15480036]
30. American College of Radiology. Liver Imaging Reporting and Data System version 2014. Accessed March 2015 from <http://www.acr.org/Quality-Safety/Resources/LIRADS>

Key points

- Ipsilateral and contralateral ROI placement produces high consistency and low variance.
- Both ROI placement methods produce qEASL values that correlate well with histopathology.
- Ipsilateral ROI placement produces best correlation to pathology along with high consistency.

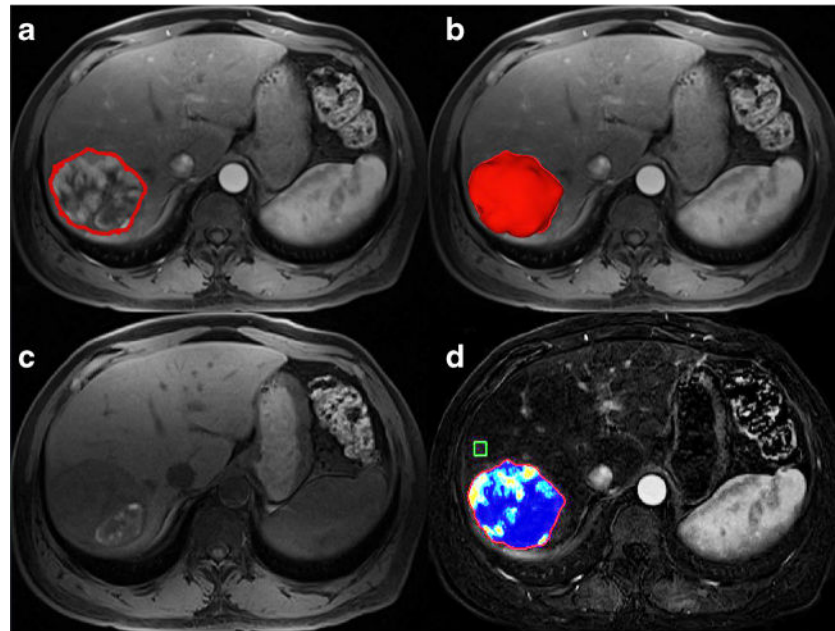


Fig. 1. 3D Quantitative Image Analysis. *A)* Representative contrast-enhanced T1-weighted MR image demonstrates semi-automatic tumour segmentation, 20 seconds after addition of contrast. *B)* Representative MR image with corresponding 3D rendering of segmented tumour. *C)* Representative MR image without contrast. *D)* Subtraction of (*A*) and (*C*) and qEASL colour map of tumour (*red* represents maximum enhancement and blue represents no enhancement)

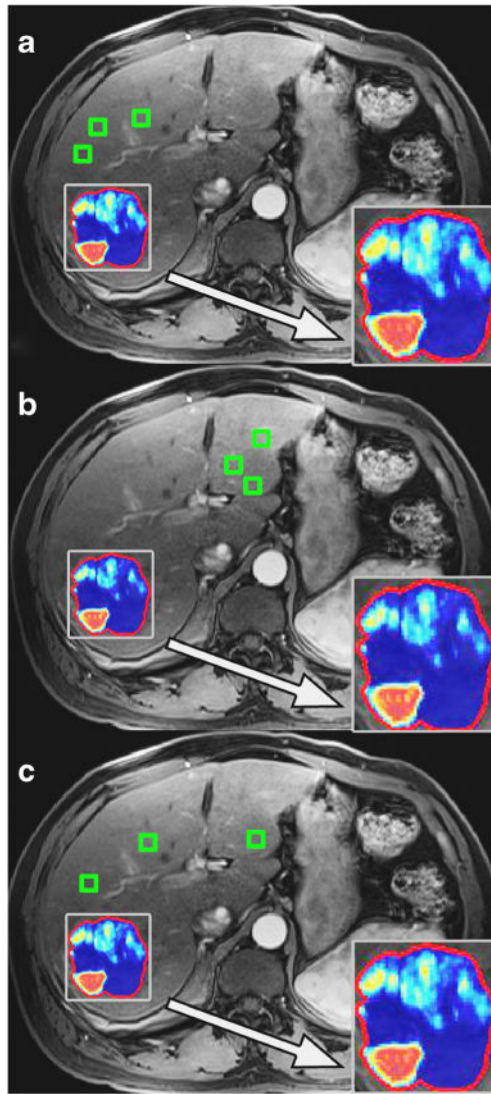


Fig. 2.
 The systematic ROI placement method in the same representative patient case as in Figure 1. *A)* Three ROIs were subsequently placed near the lesion (i.e., ipsilateral liver lobe to the lesion). *B)* Three ROIs were placed away from the lesion (contralateral liver lobe to the lesion). *C)* Three ROIs were placed dispersed throughout the liver. Representative qEASL colour maps produced from each ROI placement method is also shown in closer detail within the zoom boxes

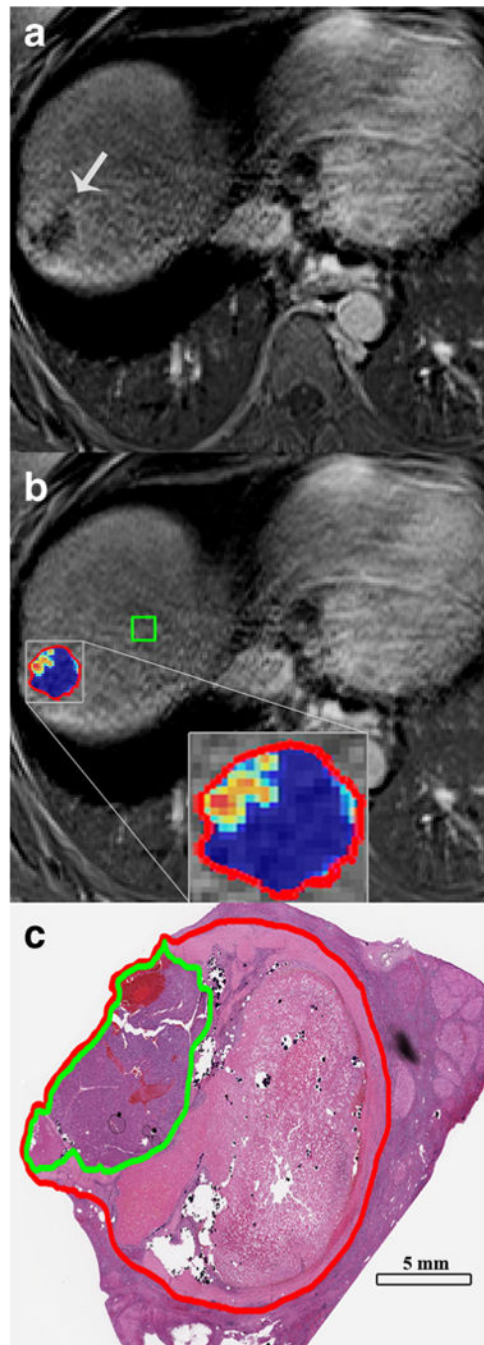


Fig. 3. qEASL correlation with pathology. *A)* Subtraction result of pre and post contrast-enhanced MR images with tumour indicated by the arrow. *B)* The above with qEASL colour map of the lesion (*red outline*) showing *blue* colour indicating necrotic regions and *red/yellow* colour indicating viable regions. This has similar distribution as seen in the photomicrograph. *C)* The histosegmentation technique of the same lesion (*red outline*) is shown with a *green outline* representing viable tumour tissue, whereas the rest of the tumour is necrotic

Variance of Systematic ROI Placement

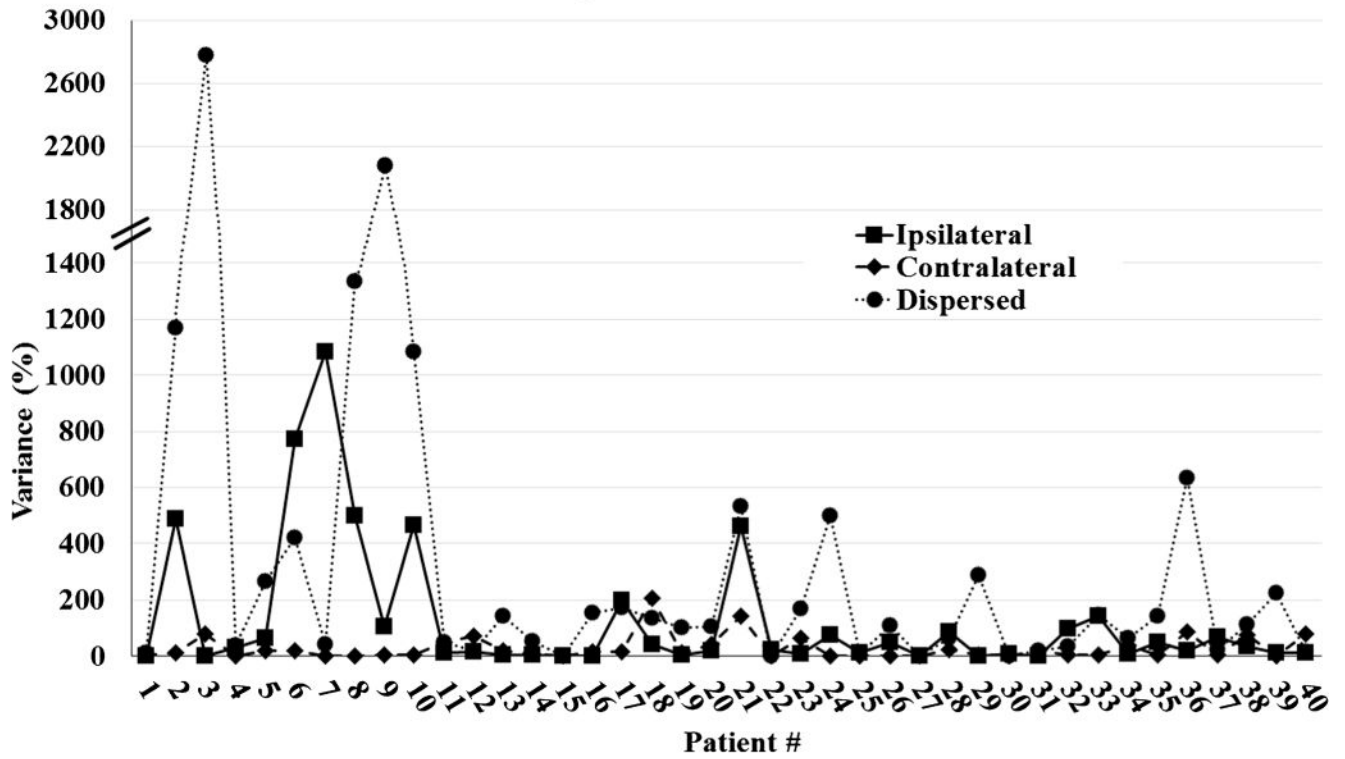


Fig. 4. Variance comparison of systematic ROI placement methods. Note that the dispersed placement method results in much greater variance than the ipsilateral and contralateral approaches

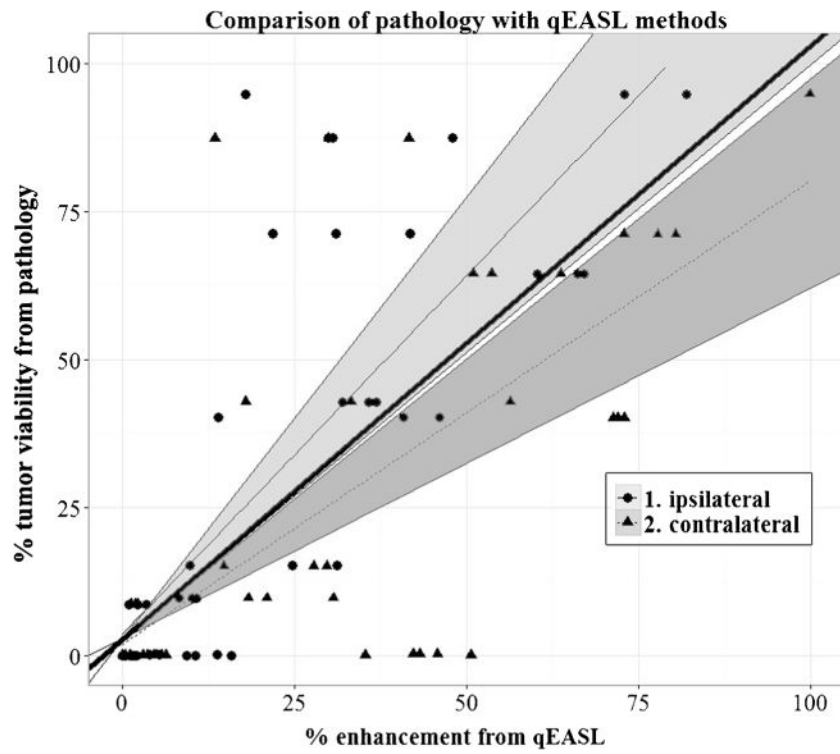


Fig. 5. Comparison of pathology with ipsilateral and contralateral ROI placement methods. Note how the 95 % confidence interval of the ipsilateral approach includes reference line with slope of 1, whereas the contralateral approach does not, indicating the ipsilateral method more closely matches with pathology (95 % confidence intervals are shaded)

Table 1

Baseline patient characteristics for Phase 1 and 2 patient cohorts

Parameter	Phase 1 N (%)	Phase 2 N (%)
<i>Demographics</i>		
Age*	65±2 (range, 39–85)	61±2 (range, 52–83)
Sex		
Male	27 (68)	13 (87)
Female	13 (32)	2 (13)
Ethnicity		
Caucasian	26 (65)	10 (66)
African American	10 (25)	4 (27)
Other	4 (10)	1 (7)
Etiology		
HBV	4 (10)	1 (7)
HCV	22 (55)	3 (20)
Alcohol abuse	8 (20)	1 (7)
HBV and HCV	0 (0)	1 (7)
HCV and Alcohol Abuse	6 (15)	7 (47)
Cirrhosis		
Present	40 (100)	15 (100)
Ascites		
Present	9 (23)	3 (20)
ECOG performance status		
0	19 (48)	11 (73)
1	20 (50)	3(20)
2	1 (3)	1 (7)
<i>Staging System</i>		
BCLC class		
A	7 (18)	2 (13)
B	6 (15)	7 (47)
C	27 (68)	6(40)
Child-Pugh class		
A	26 (65)	10 (66)
B	14 (35)	4(27)
C	0 (0)	1 (7)
<i>Tumour Characteristics</i>		
Size		
<3 cm	14 (35)	5 (33)
3–5 cm	11 (28)	6 (40)
5–7 cm	5 (13)	1 (7)
7–10 cm	6 (15)	2 (13)
>10 cm	4.(10)	1 (7)

Data represents number of patients with respective percentages in parentheses

* Data represented as mean±standard deviation. HBV, Hepatitis B Virus; HCV, Hepatitis C Virus; ECOG, Eastern Cooperative Oncology Group; BCLC, Barcelona Clinic Liver Cancer

Author Manuscript

Author Manuscript

Author Manuscript

Author Manuscript

Table 2

Single measure, one-way random, absolute agreement intra-class coefficient for consistency

	Intra-rater	Inter-Method	Temporal
Ipsilateral	0.828 ([0.731, 0.898])	0.635 ([0.522, 0.750])	0.664 ([0.388, 0.815])
Contralateral	0.971 ([0.951, 0.983])		0.118 ([-0.605, 0.515])
Dispersed	0.604 ([0.435, 0.748])		0.210 ([-0.437, 0.566])

Author Manuscript

Author Manuscript

Author Manuscript

Author Manuscript

Table 3

Average percent necrosis values as determined by qEASL

Patient	Histosegmentation on Pathology [% Necrosis]	% Necrosis Ipsilateral	% Necrosis Contralateral	% Necrosis Radiologist RS	% Necrosis Radiologist RD
1	35.51	35.5±3.7	43.9±6.7	88±7.2	74.5±4.6
2	12.65	63.8±10.3	71.7±14.2	81.6±1.3	59.9±5.9
3	99.95	99±0.5	98.5±1.3	97.8±2.8	98.3±1.7
4	99.79	92.3±5.3	56.3±1.8	82.9±7.3	91.7±3.3
5	90.3	90.3±1.4	76.7±6.5	88.8±7.8	88.6±3.2
6	84.83	78.2±11	76±8.1	88.4±10.7	72.7±5.5
7	59.85	66.5±17.3	27.9±0.8	65.7±18.6	55.9±3
8	100	88.2±3.4	54.5±8.9	78.7±15	87.1±0.7
9	100	99.2±1.1	96.8±2.7	100±0	98.8±0.2
10	100	100±0	100±0	95.7±5.4	100±0
11	100	99.9±0	94.7±1	99.8±0	99.8±0.1
12	57.12	65.1±2.6	64.2±19.3	83.8±6.3	76.6±4.2
13	5.26	42.4±34.8	0.1±0.1	70.1±41.4	13.2±7.9
14	91.32	97.9±1.3	98.3±0.5	98.5±1.1	98.9±0.1
15	28.78	68.5±10	22.9±3.8	78.6±4.9	48.7±12.7

Table 4

Radiological–pathological correlation of qEASL measurements. Regression coefficients and coefficient intervals (CI) intervals were calculated using linear regression. Correlation coefficients were calculated using the Pearson correlation test. Median difference and standard errors were calculated

	Regression Coefficient, [95 % CI]	Correlation to Pathology	qEASL [Median Difference ± Std Deviation]
Ipsilateral	1.157, [0.904, 1.409]	0.886	5.448±18.194
Contralateral	0.714, [0.543, 0.885]	0.727	8.551 ±18.818
Radiologist 1	1.293, [0.909, 1.677]	0.625	10.402±25.596
Radiologist 2	1.122, [0.887, 1.357]	0.879	7.450±14.396